

Complete Classification of the String-like Solutions of the Gravitating Abelian Higgs Model

M. Christensen^{a*}, A.L. Larsen^{a†} and Y. Verbin^{b‡}

February 7, 2008

^a *Department of Physics, University of Odense,
Campusvej 55, 5230 Odense M, Denmark*

^b *Department of Natural Sciences, The Open University of Israel,
P.O.B. 39328, Tel Aviv 61392, Israel*

Abstract

The static cylindrically symmetric solutions of the gravitating Abelian Higgs model form a two parameter family. In this paper we give a complete classification of the string-like solutions of this system. We show that the parameter plane is composed of two different regions with the following characteristics: One region contains the standard asymptotically conic cosmic string solutions together with a second kind of solutions with Melvin-like asymptotic behavior. The other region contains two types of solutions with bounded radial extension. The border between the two regions is the curve of maximal angular deficit of 2π .

PACS: 11.27.+d, 04.20.Jb, 04.40.Nr

1 Introduction

Cosmic strings [1, 2] were introduced into cosmology by Kibble [3], Zel'dovich [4] and Vilenkin [5] as (linear) topological defects, which may have been formed during phase transitions in the early universe. Cosmic strings are considered as possible sources for density perturbations and hence for structure formation in the universe.

The simplest and most common field-theoretical model, which is used in order to describe the generation of cosmic strings during a phase transition, is the Abelian Higgs model. This model is known to have (magnetic) flux tube solutions [6], whose gravitational field is represented by an asymptotically conic geometry. These are the local cosmic string solutions.

This conic space-time is a special case of the general static and cylindrically-symmetric vacuum solution of Einstein equations [7], the so-called Kasner solution:

$$ds^2 = (kr)^{2a} dt^2 - (kr)^{2c} dz^2 - dr^2 - \beta^2 (kr)^{2(b-1)} r^2 d\phi^2 \quad (1.1)$$

where k sets the length scale while β represents the asymptotic structure, as will be discussed below. Notice also that (a, b, c) must satisfy the Kasner conditions:

$$a + b + c = a^2 + b^2 + c^2 = 1 \quad (1.2)$$

*Electronic address: mc@bose.fys.ou.dk

†Electronic address: all@fysik.ou.dk

‡Electronic address: verbin@oumail.openu.ac.il

The standard conic cosmic string solution [5, 8] is characterized by an asymptotic behavior given by (1.1) with $a = c = 0$, $b = 1$ which is evidently locally flat. In this case, the parameter β represents a conic angular deficit [9, 10], which is also related to the mass distribution of the source.

A first approximation to the relation between the angular deficit $\delta\phi = 2\pi(1 - \beta)$ and the “inertial mass” (per unit length) \tilde{m} , of a local string was found to be [5, 11, 12, 13]:

$$\delta\phi = 8\pi G\tilde{m} \quad (1.3)$$

Further corrections to (1.3) were calculated in the following papers [14, 15, 16, 17, 18].

In order to fully analyse the string-like solutions of the Abelian Higgs system one needs to solve the full system of coupled field equations for the gravitational field and matter fields (scalar + vector). But this is not necessary in order to obtain the asymptotic geometry. It is sufficient to note that for cylindrical symmetry the flux tube has the property of $\mathcal{T}_0^0 = \mathcal{T}_z^z$, where \mathcal{T}_ν^μ is the energy-momentum tensor. This means that the solution will have a symmetry under boosts along the string axis, i.e., $a = c$. The Kasner conditions (1.2) then leave only two options; either the locally flat case:

$$a = c = 0 \quad , \quad b = 1 \quad (1.4)$$

which we shall refer to as the cosmic string branch, or

$$a = c = 2/3 \quad , \quad b = -1/3 \quad (1.5)$$

which is the same behavior as that of the Melvin solution [19]. We shall therefore refer to (1.5) as the Melvin branch.

The Melvin branch does not provide the same characteristics used to describe a “standard” cosmic string, and thus it has been disregarded in previous investigations. However, the Melvin-like solution seems completely well-behaved and one may wonder whether it exists at all (asymptotically), or maybe it is just an artifact of the too general reasoning above. Although several authors [17, 18, 20, 21, 22] explicitly mention this possibility of a second Melvin branch of solutions in the Abelian Higgs system, it has never been properly discussed.

In this paper we show that indeed the Melvin branch actually exists in the Abelian Higgs model. It turns out that each conic cosmic string solution has a “shadow” in the form of a corresponding solution in the Melvin branch. These two solutions, conic cosmic string and asymptotic Melvin, are found only in a part of the two dimensional parameter space of the system, bounded by the curve of maximal angular deficit of 2π .

There also seem to be some open questions in the literature [16, 20] about the nature of the solutions beyond the border of maximal angular deficit of 2π . We will see that also in this region two types of solutions coexist, both of them with a finite radial extension.

2 General analysis of the Abelian Higgs system

The action of the gravitating Abelian Higgs model is:

$$S = \int d^4x \sqrt{|g|} \left(\frac{1}{2} D_\mu \Phi^* D^\mu \Phi - \frac{\lambda}{4} (\Phi^* \Phi - v^2)^2 - \frac{1}{4} F_{\mu\nu} F^{\mu\nu} + \frac{1}{16\pi G} \mathcal{R} \right) \quad (2.1)$$

where \mathcal{R} is the Ricci scalar, $F_{\mu\nu}$ the Abelian field strength, Φ is a complex scalar field with vacuum expectation value v and $D_\mu = \nabla_\mu - ieA_\mu$ is the usual gauge covariant derivative. We use units in which $\hbar = c = 1$.

Because of the cylindrical symmetry of the source, we will use a line element of the form:

$$ds^2 = N^2(r) dt^2 - dr^2 - L^2(r) d\phi^2 - K^2(r) dz^2 \quad (2.2)$$

and the usual Nielsen-Olesen ansatz for the +1 flux unit:

$$\Phi = v f(r) e^{i\phi} \quad , \quad A_\mu dx^\mu = \frac{1}{e} (1 - P(r)) d\phi \quad (2.3)$$

This gives rise to the following field equations for the Abelian Higgs flux tube:

$$\frac{(NKLf')'}{NKL} + \left(\lambda v^2(1-f^2) - \frac{P^2}{L^2} \right) f = 0 \quad (2.4)$$

$$\frac{L}{NK} \left(\frac{NK}{L} P' \right)' - e^2 v^2 f^2 P = 0 \quad (2.5)$$

With the line element (2.2), the components of the Ricci tensor are:

$$\begin{aligned} \mathcal{R}_0^0 &= -\frac{(LKN')'}{NLK} \quad , \quad \mathcal{R}_r^r = -\frac{N''}{N} - \frac{L''}{L} - \frac{K''}{K} \\ \mathcal{R}_\phi^\phi &= -\frac{(NKL')'}{NLK} \quad , \quad \mathcal{R}_z^z = -\frac{(NLK')'}{NLK} \end{aligned} \quad (2.6)$$

The source is described by the energy-momentum tensor with the following components:

$$\begin{aligned} \mathcal{T}_0^0 &= \rho = \varepsilon_s + \varepsilon_v + \varepsilon_w + u \\ \mathcal{T}_r^r &= -p_r = -\varepsilon_s - \varepsilon_v + \varepsilon_w + u \\ \mathcal{T}_\phi^\phi &= -p_\phi = \varepsilon_s - \varepsilon_v - \varepsilon_w + u \\ \mathcal{T}_z^z &= -p_z = \rho \end{aligned} \quad (2.7)$$

where:

$$\varepsilon_s = \frac{v^2}{2} f'^2 \quad , \quad \varepsilon_v = \frac{P'^2}{2e^2 L^2} \quad , \quad \varepsilon_w = \frac{v^2 P^2 f^2}{2L^2} \quad , \quad u = \frac{\lambda v^4}{4} (1-f^2)^2 \quad (2.8)$$

It turns out to be convenient to use Einstein equations in the form ($\mathcal{T} \equiv \mathcal{T}_\lambda^\lambda$):

$$\mathcal{R}_{\mu\nu} = -8\pi G(\mathcal{T}_{\mu\nu} - \frac{1}{2}g_{\mu\nu}\mathcal{T}) \quad (2.9)$$

from which one obtains:

$$\frac{(LKN')'}{NLK} = 4\pi G(\rho + p_r + p_\phi + p_z) = 8\pi G(\varepsilon_v - u) \quad (2.10)$$

$$\frac{(NKL')'}{NLK} = -4\pi G(\rho - p_r + p_\phi - p_z) = -8\pi G(\varepsilon_v + 2\varepsilon_w + u) \quad (2.11)$$

$$\frac{(LNK')'}{NLK} = -4\pi G(\rho - p_r - p_\phi + p_z) = 8\pi G(\varepsilon_v - u) \quad (2.12)$$

and instead of the “radial” part of (2.9), we take the following combination:

$$\frac{N'}{N} \frac{L'}{L} + \frac{L'}{L} \frac{K'}{K} + \frac{K'}{K} \frac{N'}{N} = 8\pi G p_r = 8\pi G(\varepsilon_s + \varepsilon_v - \varepsilon_w - u) \quad (2.13)$$

which is not an independent equation but serves as a constraint. In vacuum, the right-hand-sides of these equations vanish, and the first three of them are trivially integrated. In this way we may get back Kasner’s line element (1.1). This is therefore the asymptotic form of the metric tensor around any (transversally) localized source and especially around an Abelian Higgs flux tube. Moreover, it is easy to get convinced that due to the symmetry under boosts along the string axis, $K = N$.

The equations become more transparent if we express all lengths in terms of the scalar characteristic length scale $1/\sqrt{\lambda v^2}$ (the “correlation length” in the superconductivity terminology). We therefore change to the dimensionless length coordinate $x = \sqrt{\lambda v^2} r$ and we introduce the metric component $L(x) = \sqrt{\lambda v^2} L(r)$. We also introduce the two parameters $\alpha = e^2/\lambda$ and $\gamma = 8\pi G v^2$. In terms of these new quantities, we get a two parameter system of four coupled non-linear ordinary differential equations (the prime now denotes d/dx):

$$\frac{(N^2 L f')'}{N^2 L} + \left(1 - f^2 - \frac{P^2}{L^2}\right) f = 0 \quad (2.14)$$

$$\frac{L}{N^2} \left(\frac{N^2 P'}{L} \right)' - \alpha f^2 P = 0 \quad (2.15)$$

$$\frac{(L N N')'}{N^2 L} = \gamma \left(\frac{P'^2}{2\alpha L^2} - \frac{1}{4}(1 - f^2)^2 \right) \quad (2.16)$$

$$\frac{(N^2 L')'}{N^2 L} = -\gamma \left(\frac{P'^2}{2\alpha L^2} + \frac{P^2 f^2}{L^2} + \frac{1}{4}(1 - f^2)^2 \right) \quad (2.17)$$

We have also to keep in mind the existence of the constraint (2.13), which gets the following form:

$$\frac{N'}{N} \left(2 \frac{L'}{L} + \frac{N'}{N} \right) = \gamma \left(\frac{f'^2}{2} + \frac{P'^2}{2\alpha L^2} - \frac{P^2 f^2}{2L^2} - \frac{1}{4}(1 - f^2)^2 \right) \quad (2.18)$$

In order to get string-like solutions, the scalar and gauge fields should satisfy the following boundary conditions:

$$\begin{aligned} f(0) &= 0 \quad , \quad \lim_{x \rightarrow \infty} f(x) = 1 \\ P(0) &= 1 \quad , \quad \lim_{x \rightarrow \infty} P(x) = 0 \end{aligned} \quad (2.19)$$

Moreover, regularity of the geometry on the symmetry axis $x = 0$ will be guaranteed by the “initial conditions”:

$$\begin{aligned} L(0) &= 0 \quad , \quad L'(0) = 1 \\ N(0) &= 1 \quad , \quad N'(0) = 0 \end{aligned} \quad (2.20)$$

The purpose of the present paper is to map the two dimensional α - γ parameter space, and thereby to classify all the string-like solutions of the Abelian Higgs system. It is well-known that, even in flat space, the field equations can only be solved numerically. However, much can be said about the nature of the solutions even without explicitly solving the field equations [8, 16, 17, 21].

The standard Abelian Higgs string solution, usually considered in the literature, has a vanishing gravitational mass. This means that the spacetime around the string is locally flat except in the core of the string, while there is a non-trivial global effect namely a conical structure of the space which is quantified by an angular deficit. However, this does not at all saturate all the possibilities of solutions of (2.14)-(2.17). There are further types of solutions with the same boundary and “initial” conditions, (2.19)-(2.20), which are not asymptotically flat but have interesting physical interpretations. In this paper, we will show that a point in the α - γ plane always represents two solutions, except at the curve representing angular deficit of 2π . The various solutions are distinguished by, among other things, their asymptotic geometries.

For analysing the solutions and obtaining the above-mentioned features and some additional ones, we introduce the Tolman mass (per unit length), M :

$$GM = 2\pi G \int_0^\infty dr N^2 L (\rho + p_r + p_\phi + p_z) = \frac{\gamma}{2} \int_0^\infty dx N^2 L \left(\frac{P'^2}{2\alpha L^2} - \frac{1}{4}(1 - f^2)^2 \right) \quad (2.21)$$

Using the field equations, one can show that [18]:

$$GM = \frac{1}{2} \lim_{x \rightarrow \infty} (L N N') \quad (2.22)$$

We also define the magnetic field B :

$$B = -\frac{1}{eL(r)} \frac{dP(r)}{dr} = -\frac{\gamma}{\alpha} \left(\frac{e}{8\pi G} \right) \frac{P'(x)}{L(x)} \quad (2.23)$$

and the dimensionless parameter $\mathcal{B} = 8\pi GB(0)/e$. We find that the central value of the magnetic field (its value in the core of the string) can be expressed as [18]:

$$\mathcal{B} = 1 + 2GM - \lim_{x \rightarrow \infty} (N^2 L') \quad (2.24)$$

The asymptotic form of the metric tensor is easily found by direct integration of the two Einstein equations (2.16)-(2.17) using the boundary conditions and the definitions of M and \mathcal{B} . It is of the Kasner form

$$N(x) = K(x) \sim \kappa x^a, \quad L(x) \sim \beta x^b \quad (2.25)$$

with:

$$a = \frac{2GM}{6GM + 1 - \mathcal{B}}, \quad b = \frac{2GM + 1 - \mathcal{B}}{6GM + 1 - \mathcal{B}}, \quad \kappa^2 \beta = 6GM + 1 - \mathcal{B} \quad (2.26)$$

The constant κ appears free in the asymptotic solution, but it is uniquely fixed in the complete one by the boundary conditions on the metric.

Due to (2.18) we get the following relation which is equivalent to the quadratic Kasner condition in Eq. (1.2):

$$GM(3GM + 1 - \mathcal{B}) = 0 \quad (2.27)$$

This immediately points to the possibility of two branches of solutions corresponding to the vanishing of either factor in Eq. (2.27). These two possibilities of course represent the two branches already discussed in Section 1.

Consider first the cosmic string branch ($a = c = 0$, $b = 1$) in a little more detail. In this case, we find a simple physical interpretation to the parameters in Eq. (2.25). the constant $\beta = L'(\infty)$ defines the deficit angle $\delta\phi = 2\pi(1 - \beta)$, while the constant $\kappa = N(\infty)$ is the red/blue shift of time between infinity and the string core. Moreover, relations (2.22), (2.24) give:

$$M = 0 \quad (2.28)$$

$$\mathcal{B} = 1 - \kappa^2 \left(1 - \frac{\delta\phi}{2\pi}\right) \quad (2.29)$$

That is to say, the Tolman mass vanishes and the central magnetic field is directly expressed in terms of the red/blue shift κ and the deficit angle $\delta\phi$.

Then consider the Melvin branch ($a = c = 2/3$, $b = -1/3$). In this case there is no simple physical interpretation of the parameters β and κ in Eq. (2.25). As for the Tolman mass, we notice that it is non-zero, but the equations (2.22), (2.24) lead to a simple relation to the central magnetic field [18]:

$$\mathcal{B} = 1 + 3GM \quad (2.30)$$

For more discussion of these general relations (and some other ones), we refer to Ref. [18]. In the remaining sections of this paper, we shall construct explicitly the various types of solutions to (2.14)-(2.17) by using a relaxation procedure to solve the four coupled differential equations numerically. The constraint (2.18) has been used for estimating the numerical errors.

3 Open solutions: Cosmic strings and Melvin branch

The existence of cosmic string solutions in the Abelian Higgs system is very well established. However, the existence of the solutions of the second type, i.e. the Melvin branch type which is implied by (1.5) and (2.27), has not been properly studied. We have found that for any conic cosmic string solution, an associated solution exists in the Melvin branch. The main difference with respect to the cosmic string branch is the fact that asymptotically the azimuthal circles have vanishing circumference. A

related difference is the non-vanishing total mass (per unit length) of the Melvin-like solutions. Figure 1 shows an example of the conic and the Melvin-like solution at the point $(\alpha, \gamma) = (2, 1.8)$ in parameter space. Only the (square root of the) metric components, N and L , are plotted, as the scalar and vector fields for the various solutions deviate only very little from the standard and well examined cosmic string configuration. The two branches are obviously quite different. The cosmic string spacetime is asymptotically flat as N is constant (actually $N = 1$ here as $\alpha = 2$ is the Bogomol'nyi limit [23, 24]) and L becomes proportional to x far from the core. In contrast hereto, the associated solution in the Melvin branch has $N \propto x^{2/3}$ and $L \propto x^{-1/3}$ in the asymptotic region. Therefore the circumference of circles lying in planes perpendicular to the core with $x = 0$ as center will eventually decrease as one moves to larger x .

The curves shown in Figure 1 are representative for the cosmic string and Melvin branches. In the first case, increasing γ at fixed α will simply shift N towards a higher constant value in the asymptotic region, whereas L will become less steep (meaning larger angular deficit). An increase of α when γ is held constant will have the opposite effect, i.e. shifting L to lower asymptotic values and decreasing the angular deficit. This observation holds for all solutions (including the cylindrical solutions and the closed solutions to be described in Section 4): only the γ/α ratio seems to matter for the asymptotic behavior. Still, because of the region near the core, no obvious symmetry is observed that could render the parameter space effectively one dimensional. In the case of the Melvin branch, an increased γ (again at fixed α) tends to flatten N , whereas the global maximum of L takes a larger value at higher x .

Moving towards more massive strings in the parameter space (larger γ to α ratio) the angular deficit of the conic solution will increase until it reaches a maximum of 2π . The corresponding solution represents an asymptotically cylindrical manifold with N and L both asymptotically constant. One such solution exists for any α and the curve $\gamma_*(\alpha)$, where $\delta\phi = 2\pi$, plays a very special role in the classification of the various solutions. First of all, it obeys a power law [16]. Secondly, as one approaches a point on this curve in parameter space along the Melvin branch the solution converges to the same cylindrical solution as for the cosmic string; that is, the conic solutions and the Melvin-like solutions coincide in a single asymptotically cylindrical solution on the curve of maximal angular deficit.

Figure 2 illustrates how the central magnetic field \mathcal{B} varies throughout the parameter space for both the cosmic string and the Melvin-like universes. Notice how the two surfaces intersect along the curve of maximal angular deficit, where the two branches coincide in the cylindrical solutions.

4 Closed solutions: Inverted cone and singular Kasner solutions

The issue of “supermassive cosmic strings” in the Abelian Higgs system was discussed at early days [16, 20]. Two types of closed solutions were found. One [16] in which $N(x)$ vanishes at a finite distance from the axis ($x = x_{max}$) while $L(x)$ diverges at that point. In the other, $N(x)$ stays finite for any x while $L(x)$ decreases linearly outside the core of the string, and vanishes at a finite distance from the axis. The geometry is still conic but of an inverted one where the apex of the cone is at the point where $L = 0$ [11, 20]. Using the same numerical methods as in the previous section, we have found that these two types of solutions are encountered just as the curve $\delta\phi = 2\pi$ is traversed. But the lack of asymptotic behavior for closed solutions forces us to replace the boundary conditions (2.19) by the condition

$$\begin{aligned} f(0) &= 0 & , & & f(x_{max}) &= 1 \\ P(0) &= 1 & , & & P(x_{max}) &= 0 \end{aligned} \tag{4.1}$$

This ensures that the solutions are unit flux tubes, and makes the numerical work simpler. For quite large radial extension this technicality is not of any relevance as the variables f and P describing the scalar and vector fields, respectively, converge quite fast to their values at “infinity”.

Figure 3 shows an example of both kinds of solutions at the point $(\alpha, \gamma) = (2, 2.05)$ in parameter space. This is just above the curve of maximal angular deficit, which lies at $\gamma_*(2) = 2$ for fixed $\alpha = 2$,

and the solutions still have considerable sizes. Strictly speaking, these two types of solutions have no asymptotic behavior as they are both representing closed solutions that pinch off at a finite radial extension (x_{max}). But for slightly supermassive configurations we have

$$N(x) = K(x) \sim \kappa(x_{max} - x)^a \quad , \quad L(x) \sim \beta(x_{max} - x)^b \quad (4.2)$$

The inverted cone behaves according to Eq. (1.4) and the singular Kasner solution behaves according to Eq. (1.5).

The curves shown in Figure 3 are representative for the solutions above the curve of maximal angular deficit. As γ increases (α fixed) both solutions become smaller in radial extent. For the inverted cone N gets shifted to a lower constant value and L intersects zero at smaller x . Likewise x_{max} decreases for the singular Kasner solution causing L to diverge at similarly low x . We have found that for any given α and $\gamma > \gamma_*(\alpha)$, the solution with geometry as an inverted cone has the larger size.

As mentioned, the solutions shrink when γ is increased (α fixed). At some point the spacetime described by the solution becomes smaller than a few times the characteristic core thickness which scales as $\alpha^{-1/2}$ [6]. At even higher values of γ the choice of boundary conditions becomes more and more important to fundamental questions as flux quantization and topological stability; the solutions exist mathematically but are probably unphysical.

Figure 4 shows three curves in parameter space which have all been fitted to a power law, $\gamma = c_1 \alpha^{c_2}$. The lowest one is simply the curve of angular deficit 2π . This curve separates the two open solutions from the two closed ones, and represents itself a linear family of asymptotically cylindrical solutions. The middle one represents the curve in parameter space where the singular Kasner-like solutions have a radial extent of $10\alpha^{-1/2}$, i.e. ten times the characteristic thickness of the core. Similarly, the upper one represents the curve where the inverted cone solutions pinches off at $x_{max} = 10\alpha^{-1/2}$. Starting on one of these two curves and moving downwards (towards lower γ for fixed α), the two closed solutions will become more and more similar and will eventually coincide in the cylindrical solution. Moving upward instead will yield rather small and increasingly unphysical solutions.

5 Conclusion

Cylindrically symmetric configurations of the gravitating Abelian Higgs model have been examined by application of relaxation techniques to Einstein equations which simplify in this case to a system of coupled ordinary differential equations. Everywhere in parameter space two kinds of solutions exist, except at the curve of angular deficit 2π , where only one cylindrical solution exists. The two open solutions are the standard asymptotically conic cosmic string and a solution with a Melvin like asymptotic behavior. The two closed solutions are the inverted cone and a singular Kasner-like solution. Supermassive solutions pinch off very fast and are probably unphysical.

Here only the unit flux tube, $n = 1$, has been considered, but introduction of an arbitrary $n \neq 0$ is expected to give similar families of solutions, which can be examined in an analogous way.

Finally, it is worthwhile noting that the singularities of static field configurations generally seem to be lifted when time-dependence is reintroduced [25]. Therefore the nature of the singularities of the supermassive strings may be understood in the framework of time dependent analysis.

References

- [1] A. Vilenkin and E.P.S. Shellard, “*Cosmic strings and other Topological Defects*” (Cambridge Univ. Press, Cambridge, 1994).
- [2] T.W.B Kibble and M. Hindmarsh, Rep. Progr. Phys. **58**, 477 (1995).
- [3] T.W.B Kibble, J. Phys. **A9**, 1387 (1976).

- [4] Ya. B. Zel'dovich, Mon. Not. R. Astron. Soc. **192**, 663 (1980).
- [5] A. Vilenkin, Phys. Rev. **D23**, 852 (1981).
- [6] H.B. Nielsen and P. Olesen, Nucl. Phys. **B61**, 45 (1973).
- [7] D. Kramer, H. Stephani, E. Herlt and M. MacCallum, "*Exact Solutions of Einstein's Field Equations*" (Cambridge Univ. Press, Cambridge, England 1980).
- [8] D. Garfinkle, Phys. Rev. **D32**, 1323 (1985).
- [9] L. Marder, Proc. Roy. Soc. London A **252**, 45 (1959).
- [10] W.B. Bonnor, J. Phys. A **12**, 847 (1979).
- [11] J.R. Gott, Astrophys. J. **288**, 422 (1985).
- [12] W.A. Hiscock, Phys. Rev. **D31**, 3288 (1985).
- [13] B. Linet, Gen. Relativ. Gravit. **17**, 1109 (1985).
- [14] P. Laguna-Castillo and R.A. Matzner, Phys. Rev. **D36**, 3663 (1987).
- [15] D. Garfinkle and P. Laguna, Phys. Rev. **D39**, 1552 (1989).
- [16] P. Laguna and D. Garfinkle, Phys. Rev. **D40**, 1011 (1989).
- [17] J. Colding, N.K. Nielsen and Y. Verbin, Phys. Rev. **D56**, 3371 (1997).
- [18] Y. Verbin, "*Cosmic Strings in the Abelian Higgs Model with Conformal Coupling to Gravity*", preprint hep-th/9809002, to appear in Phys. Rev. **D**.
- [19] M.A. Melvin, Phys. Lett. **8**, 65 (1964).
- [20] M.E. Ortiz, Phys. Rev. **D43**, 2521 (1991).
- [21] V.P. Frolov, W. Israel and W.G. Unruh, Phys. Rev. **D39**, 1084 (1989).
- [22] A.K. Raychaudhuri, Phys. Rev. **D41**, 3041 (1990).
- [23] B. Linet, Phys. Lett. A **124**, 240 (1987).
- [24] A. Comtet and G.W. Gibbons, Nucl. Phys. **B299**, 719 (1988).
- [25] I. Cho, Phys. Rev. **D58**, 103509 (1998).

Figure 1: Typical examples of the numerical solutions at low γ . Here, at the point $(\alpha, \gamma) = (2, 1.8)$ in parameter space, two solutions coexist. The shown metric components N and L are for the cosmic string branch and the Melvin branch respectively. Both solutions are open and seem well behaved according to Eqs. (1.4) and (1.5).

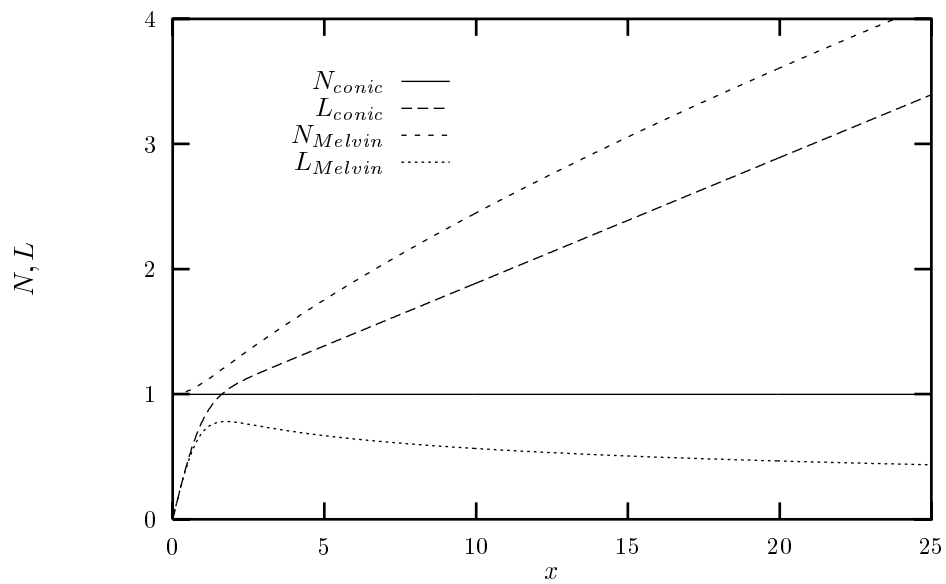


Figure 2: The central magnetic field at the string core plotted for both the cosmic string and the Melvin branch. As γ is increased (for fixed α), the solutions in the two branches will converge towards the same cylindrical solution causing the two surfaces to intersect at the curve of angular deficit $\delta\phi = 2\pi$.

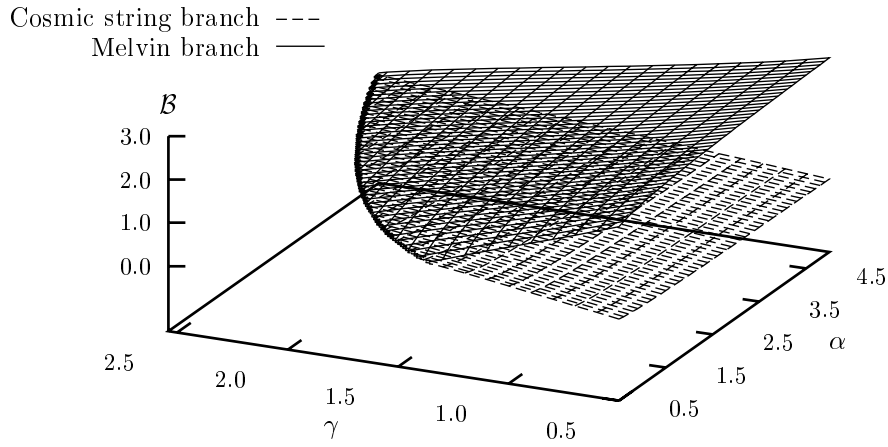


Figure 3: Typical examples of the super-massive solutions. Again two different solutions coexist, here at $(\alpha, \gamma) = (2, 2.05)$ which is above the curve of maximal angular deficit. Both the inverted cone and the Kasner solutions represent closed solutions, and for the Kasner-like solution L has a singularity at x_{max} where $N = 0$.

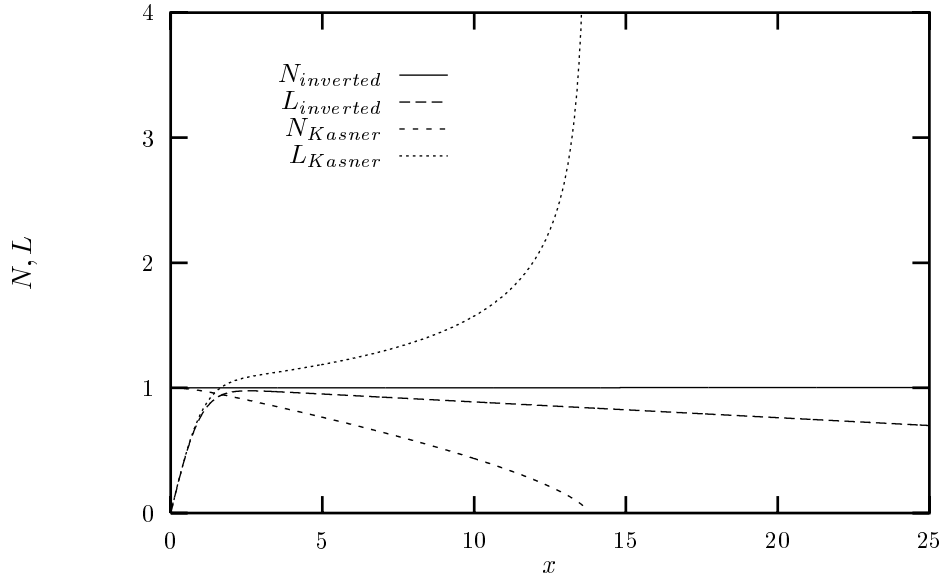


Figure 4: Just above the curve of maximal angular deficit, which represents the cylindrical solutions (lower curve), two closed solutions coexist. As γ is increased (fixed α) the radial extent of these solutions decreases. The middle and upper curve represents respectively the singular Kasner-like and the inverted cone solutions with sizes of ten times the characteristic core thickness. Above these two curves the solutions become unphysical. Notice that the three curves can be fitted to power laws; lower: $c_1 \approx 1.64 \wedge c_2 \approx 0.275$, middle: $c_1 \approx 1.72 \wedge c_2 \approx 0.285$ and upper: $c_1 \approx 1.87 \wedge c_2 \approx 0.330$.

